Bubble induced shear stress in flat sheet membrane systems – Serial examination of single bubble experiments with the electrodiffusion method

Lutz Böhm*[a], Anja Drews[b], Matthias Kraume[a]
[a]Technische Universität Berlin, Chair of Chemical and Process Engineering, FH6-1, Fraunhoferstrasse 33-36, 10587 Berlin, lutz.boehm@tu-berlin.de
[b]HTW Berlin University of Applied Science, Engineering II, School of Life Science Engineering, Wilhelminenhofstr. 75A, 12459 Berlin, anja.drews@htw-berlin.de
*corresponding author: phone: +49/30/314-72791, fax: +49/30/314-21134

Abstract

With regard to the improvement of the cleaning process of flat sheet membrane modules by aeration, a statistical analysis of the shear stress generated by single bubbles is shown for 21 different parameter combinations of varied channel depths, bubble sizes and liquid velocities. A fully automated rig allowed the generation of a sufficient database of shear stress data gained with the electrodiffusion method (EDM). The maximum shear stresses and the global shear stress levels, where the latter represent the global shear stress fluctuations, were determined. To the authors' knowledge, for the first time in membrane research a transient correction of the EDM data was performed which is necessary in cases of highly transient processes. By showing different probability ranges gained from cumulative distribution functions in bar plots, a way of presenting the data was introduced that simplifies the comparison between the different geometrical and operating parameter combinations. Additionally, this type of diagram offers a very comprehensive overview of the measured data. Both the maximum shear stress and the global shear stress level are larger when the bubble is larger than the channel depth and when an additional liquid velocity is superimposed. In all cases, the transient correction yielded higher values. Thus it is necessary to take this measure.

In the investigated range, the highest maximum values were obtained for the case with superimposed liquid velocity, a channel depth of 5 mm and a bubble size of 9 mm with appr. 1.3 Pa (steady analysis) or 4.7 Pa (transient corrected analysis), respectively. The largest fluctuation ranges of the global shear stress level were obtained for a channel depth of 5 mm and a bubble size of 9 mm with values from appr. 0.2-1.1 Pa (steady analysis) or 0-2.6 Pa (transient corrected analysis), respectively.

Keywords

Flat sheet membrane module, bubble, shear stress, electrodiffusion method

Nomenclature

I – current [A]

k_{Cot} – Cottrell coefficient [$As^{1/2}$]

k_{Lev} – Leveque coefficient [A/s]

t – time [s]

μ - dynamic viscosity [Pas]

τ – shear stress [Pa]

τ_c – transient corrected shear stress [Pa]

1. Introduction

Aeration is an operation widely used in membrane filtration. Besides supplying oxygen it is mainly used because of its cleaning effect. The rising bubbles induce liquid flows and in turn shear stresses which are responsible for the shear forces that can detach deposition layers from the surfaces. Despite the largely different types of modules and different membrane geometries that are used in membrane bioreactors (MBR[1]), the principle of air scouring is widely applied. Since the multiphase flows in commonly used module types (flat sheets, hollow fibres or tubular) differ strongly, they cannot be described by a joint model. Thus, this work focusses only on flat sheet membrane modules. Looking at commercial systems it is obvious that neither design nor operation have been systematically optimized yet [1]. Therefore, it is necessary to investigate such systems fundamentally to get a deeper insight into the cleaning process. This work's approach is to investigate the shear stresses generated by a single bubble in a single rectangular channel. This rather academic approach is chosen because changing one parameter in the real system with a bubble swarm in a flat sheet membrane module will have several effects due to the complex interactions between water, bubbles, module and tank. Without knowing fundamentals of the bubble behavior in such systems it will be impossible to interpret the results.

To the authors' knowledge, no comprehensive fundamental investigation of the rise of single bubbles in rectangular channels where the bubble size is in the range of the channel depth has been reported yet. The parameters varied in this study are the bubble size, the channel depth and - with regard to the air lift loop effect in real MBRs – the superimposed liquid velocity. The technique to measure the shear stress chosen in this project is the electrodiffusion method (EDM). This measurement technique was used for the investigation of membrane systems of all geometries in the past [2]. Bérubé's group applied the technique to hollow fibre and tubular membrane systems [3-10] where the investigated systems ranged from single membranes to full size modules. They observed the strong influence of the two-phase flow in general on the shear stress with fluctuations even leading to flow reversal induced by the bubbles. In particular they investigated the influence of bubble size and frequency, fibre packing density, fibre swaying and viscosity. Cabassud's group [11, 12] applied EDM to a single rectangular channel. In their rather small test cell (147 mm height) they observed a non-uniform shear stress distribution. Zhang et al. [13] varied parameters such as air flow rate, bubble size and bubble frequency. Their experimental rig had a rather large depth (20 mm) which is not applied in real flat sheet systems. Nevertheless, they found a strong influence of the varied parameters on the occurring shear stress. Gaucher et al. [14-18] also used an experimental rig with a rather small height of 122 mm but still performed the most comprehensive investigations regarding flat sheet systems. They varied

[1] CDF: Cumulative Distribution Function, CFD: Computational Fluid Dynamics, EDM: Electrodiffusion Method, MBR: Membrane Bioreactor

the channel depth, liquid distributor shapes, viscosity and flux. They found that fluctuating shear stress has a positive effect on the cleaning. Regarding all these publications, it is still not clear yet what the most important factor regarding the shear stress is. Potential factors are the maximum value, the average value, frequency of the fluctuations etc. All of these might be optimal for different constructional and operational conditions. For both, the designer and the operator, however it is essential to know if, e.g., a higher maximum shear stress or a different frequency etc. will mitigate fouling as these can be influenced e.g. by different types of sparging.

Here, for the first time a fully automated rig was used which allows fully developed flows, a variable depth in the range of real flat sheet membrane systems, the possibility to generate bubbles of defined sizes and the ability to establish defined superimposed liquid flows. The automation permits to produce a statistically sufficient amount of data for each parameter combination. Finally, the data is analyzed regarding the maximum occurring shear stress and the fluctuations of the shear stress as both factors seem to be crucial for the cleaning process.

2. Materials and Methods

2.1. Apparatus

The three parameters channel depth (3-7 mm), bubble size (expressed as the equivalent spherical diameter, 3-9 mm) and superimposed liquid velocity (0-20 cm/s) based on typical values [1] were chosen to be varied in this investigation (Tab. 1). One rectangular acrylic glass channels with a variable depth was constructed. The depth was set by including a certain number of PVC-sheets with a defined thickness (Fig. 1a). The width is 160 mm and the height is 1000 mm. At the bottom of the channel the needle of a 50 ml Hamilton Gastight® syringe can be inserted into the channel through a septum. The syringe is operated with a Harvard Apparatus Pump 11 Elite™ syringe pump which injects a specific volume of gas into a small cup which is fixed on a revolving rod. This can be turned with a servo motor which again is located outside of the channel. Additionally, inlets are located at the bottom of the channel through which liquid is introduced with a defined volumetric flow rate.

The system is automated with NI LabView™ so that the whole process of establishing a defined liquid volumetric flow rate, inserting a bubble of a defined size, releasing a bubble and recording the measurement data works in an automated mode (Fig. 1b). The automation is necessary to generate the amount of data necessary for the statistical analysis. For the experiments reported here, approximately 1500 single bubble rises were recorded for each parameter combination to get statistically relevant results. This took 3 to 5 days for each combination.

2.2. Electrodiffusion method

2.2.1. Working principle

The EDM works on an electrochemical principle [19]. For the EDM, basically two electrodes and an electrolyte solution between these two are necessary. Usually a very small cathode mounted flush with the wall where the measurements are taken and an anode (e.g. stainless steel) with a much larger surface is used. The anode or counter-electrode may be a specially added electrode or a (e.g. stainless steel) part of the experimental rig. Furthermore the electrolyte solution usually consists of water, two types of ions which differ only by their valence and inert ions. When applying a voltage between the cathode and the anode, a heterogeneous reaction takes place at cathode and anode in which oxidizing ions take up an electron at the cathode. Transfer of the oxidizing ions to the cathode and the electron exchange leads to charge equalization between anode and cathode which induces a measurable current. The higher the mass transport of the ions, the higher the measured value of the current. Therefore, since the rate of mass transfer of ions at the cathode is directly related to the hydrodynamic conditions in the proximity of the cathode in the system, the magnitude of current induced at the cathode can be used to measure shear stress. The well-known Leveque equation [19] is used to correlate the measured current to the shear stress

$$\tau = \mu \frac{I^3}{k_{Lev}^3} \qquad (1)$$

where τ is the shear stress in Pa, μ is the dynamic viscosity in Pas, I is the current in A and k_{Lev} is the Leveque coefficient in A^3s^{-1}. To be precise, this correlation is only valid for steady flows and flows with slow fluctuations. Besides others, e.g. Sobolik et al. [20] suggest a correction of the correlating function for transient flows

$$\tau_c = \mu k_{Lev}^{-3} \left(I^3 + 2\, k_{Cot}^2 \frac{\partial I}{\partial t} \right) \qquad (2)$$

where τ_c is the transient corrected shear stress in Pa, k_{Cot} is the Cottrell coefficient in $As^{0.5}$ and t is the time in s. There are several possibilities to correct the shear stress [21] of which none can claim to be completely accurate. Therefore, we show the results calculated with equation (1) as well as the corrected transient results calculated with Sobolik's approach as it proved to be applicable in the past [22]. It is worth mentioning that none of the publications about the application of EDM in membrane systems mentioned above applied any correction of the signal but just used equation (1).

2.2.2. EDM measurement in practice

The electrical circuit of the EDM system consists of a voltage source, the anode and cathode in the electrolyte, a resistor and an amplifier [23]. In the system, eight parallel circuits with resistors of 100 Ω each and an amplification with a factor 1000 are used. Approximately 600 mm above the bubble inlet, the 8 cathodes (0.5 mm platinum wires mounted flush with the wall) are arranged horizontally with a distance of 5 mm to each other which ensures that the measured signals do not affect each other. The signal is recorded with a frequency of 500 or 750 Hz.

2.2.3. Calibration

As can be seen in equation (1), a calibration of the system is necessary to calculate the Leveque coefficient k_{Lev}. There are three ways to get the Leveque coefficient: a theoretical equation, a semi-empirical equation (both can be found in [19]) and a determination based on an experimental calibration. The first two are both rather unreliable as system parameters such as electrode size and ion concentration are part of the equations which cannot be determined precisely. For the experimental calibration a known shear rate needs to be established at the electrodes which can be correlated to the measured current with the help of equation (1). As even with a steady flow the Leveque coefficient can change significantly over time due to e.g. temperature or ion concentration changes in the electrolyte solution, this should be done regularly if possible. For the parameter combinations with superimposed liquid velocity this was included in the analysis of the data. For every single bubble rise event, data was recorded when the bubble did not influence the flow and the Leveque coefficient for every single run and every single electrode was calculated and used for the analysis of the data that was influenced by the bubble. For the parameter combinations without liquid velocity this ongoing calibration was not possible. Therefore, averaged values of experiments with liquid velocity were used as Leveque coefficients as the overall values were fairly constant over the duration of the parameter study.

For the analysis of the data with the help of equation (2), the Cottrell coefficient k_{Cot} has to be determined as well. The coefficient can be determined by analyzing the data of a voltage step experiment [19]. These calibration experiments were done twice on every test day with each times five runs. An average coefficient was then calculated for every single sensor.

2.3. Analysis of the data

For every single bubble rise event, a maximum shear stress value and the global shear stress level were determined using MATLAB®. Rheological tests done at the author's chair and also data published in [15] showed that the dynamic viscosity of the electrolyte is comparable to the one of water in the investigated range. Therefore, $\mu=10^{-3}$ Pas was used in the following to calculate the shear stress. For the analysis of the global shear stress level, the sensor with the peak value and the data from the two neighboring sensors were used. A time interval starting from 0.5 s before the peak value and ending 1.5 s after the peak value was taken into account as this is the range of the strongest influence of the bubble on the flow (Fig.2a).

From this data of approximately 1500 single runs per parameter combination the median value and the cumulative distribution functions (CDFs) of the maximum value were determined (Fig.2b). Based on the generally occurring shear stress, CDFs were created as well (Fig.2c). For easier comparison reasons, all CDFs were split up into different probability ranges as shown by the colored horizontal bars. These probability ranges are used in the following to compare the different parameter combinations.

Reproducibility tests for selected parameter combinations showed for the CDFs of the global shear stress level a relative difference of shear stress values at selected quantile values of generally less than 10%.

3. Results & Discussion

3.1. Maximum shear stress

Figures 3a (without superimposed liquid velocity) and 3b (with superimposed liquid velocity v_L) show the median values of the maximum shear stress and their occurrence in the CDF as described in Fig.2b for every parameter combination that was tested with the data being processed using equation (1).

Only results for stable bubbles are shown. For parameter combinations without superimposed liquid velocity and a bubble-size-to-channel-depth ratio of 3 and for combinations with superimposed liquid velocity and a bubble-size-to-channel-depth ratio greater than 2 it was not possible to generate stable bubbles. Almost all bubbles broke into two or more separate bubbles. As it was not part of this investigation these numbers cannot be seen as statistically confirmed limits for stable bubbles in rectangular channels. The ratio limits are just empirical values from observations of trial runs.

The type of diagram was chosen due to one practical aspect of EDM that needs to be considered in the interpretation which is the probability that the actual maximum shear stress occurs where one of the sensors is located. As mentioned before, the sensors have a certain distance to each other which is a necessity of the measurement technique. There are several cases when the actual maximum value will not be recorded due to this fact. It is possible that bubbles that are smaller than this distance pass the sensor array between two sensors. Bubbles larger this distance may have maximum shear stress values on a very small area which can be located between two sensors. For cases with bubble sizes equal or larger than the channel depth two-dimensional oscillation lateral to the wall are apparent. In contrast, for the cases with smaller bubbles a three-dimensional oscillation with a movement normal to the wall is apparent as well. As the sensors are only located on one side of the channel this will in itself lead to a certain fluctuation of the measured values as the bubble is not always in the same phase of its rising period i.e. it does not always have the same distance from the wall when it passes by the sensor array. This problem cannot be avoided as the beginning of the oscillation is a random process. With the high number of test runs for each parameter combination it is ensured that despite of these facts, the probability is high that actual occurring maximum shear stress values were recorded. These might not be represented by the median values but rather by the upper limits of the probability ranges. Therefore, the presented diagrams give the opportunity to get a more comprehensive overview over the range of occurring maximum shear stress values.

In Fig.3a a general trend cannot be seen. Roughly, it can be stated that with increasing bubble size and smaller channel depth the maximum shear stress values increase as well. In most cases the increase of the median values for a constant channel depth and increasing bubble size is enhanced when the equivalent bubble diameter is larger than the channel depth.

Trends are more obvious in Fig.3b for the cases with superimposed liquid velocity. Generally, with decreasing channel depth, increasing bubble size and increasing superimposed liquid velocity the median of the maximum shear stress tends to increase as well. This is an expected trend as with decreasing channel depth and increasing bubble size the grade of confinement for the bubble rises.

For the combinations with superimposed liquid velocity the slope of the median with increasing bubble size is fairly stable starting with the value generated by the single phase flow.

Furthermore, it can be stated that in most cases the sum of the shear stress of the single phase liquid flow and the maximum shear stress of the bubble rising in stagnant water is not equal to the value of the two-phase flow but generally higher which confirms findings with computational fluid dynamics

(CFD) [1]. This is due to changes in the bubble behavior with superimposed liquid velocity in comparison to its behavior in stagnant water. Besides the acceleration effect due to the liquid velocity, the shape and therefore the liquid film thickness between the bubble and the wall changes. Unpublished CFD results showed that the film thickness increases with increasing liquid velocity, that the oscillation amplitude reduces and the liquid tends to flow around the unconfined sides of the bubble and not in the liquid film. Furthermore, the region of the maximum shear stress is rather in the wake of the bubble than in the liquid film. The triplication of the sum of the shear stress of the single phase liquid flow and the bubble rising in stagnant water mentioned by Prieske et al. [1] cannot be confirmed by the experimental values. The two-phase flow values are in the range of twice of the sum. The highest median values found here are around 1.4 Pa for a 7 mm channel depth and 9 mm bubble without liquid velocity (using a linear interpolation between a bubble size of 7 mm and 10 mm for the CFD data in [1], for this parameter combination the numerical and experimental maximum shear stress values are equal) and a 5 mm channel depth and 9 mm with superimposed liquid velocity. In [1] the highest maximum shear stress value (4.3 Pa) was found for the parameter combination of a 5 mm bubble in a 3 mm channel with superimposed liquid velocity. The significance of this parameter combination cannot be confirmed. The practical issues related to the EDM mentioned above are a possible explanation why the median of the maximum shear stress values shown here are smaller than the ones Prieske et al. [1] obtained from the CFD simulations although it is worth mentioning that the values are close to the values found by Ndinisa et al. [24].

Figure 4a (without superimposed liquid velocity) and 4b (with superimposed liquid velocity) show the median values of the maximum shear stress and their occurrence in the CDF as described in Fig.2b for every parameter combination that was tested with the data being processed using equation (2) (transient corrected analysis). Generally the median values are higher in comparison to the data being processed using equation (1) (steady analysis) by a factor of two to three and the probability ranges are larger by a factor of up to six. The results are in the same range as the values found for bubble swarms by Ducom et al. [11]. The medians or at least the upper limits of the probability ranges are closer to the values found in Prieske et al. [1], some even fit the CFD values very well with only a minor difference. The findings of Prieske et al. [1] and Zhang et al. [13] of maximum shear stress values that level with increasing bubble size cannot be confirmed by this work but further investigations of other parameter combinations might be necessary. Bérubé’s group found for hollow fibre systems peak values of up to 6.83 Pa [3] and more than 10 Pa [5], respectively.

3.2. Global shear stress level

Figures 5a (without superimposed liquid velocity) and 5b (with superimposed liquid velocity v_L) show the median values of the generally occurring shear stresses and their occurrence in the CDF as described in Fig.2c for every parameter combination that was tested with the data being processed using equation (1).

All the shear stresses in Fig.5a are generated solely by the flow induced by the bubble. Therefore, all the probability ranges start at a value of 0 Pa. In Fig.5b the shear stress generated by the single phase liquid flow can be seen as a lower limit. Regardless of the bubble size all CDFs of one channel depth are equal in the range lower than this limit. With and without superimposed liquid velocity it is obvious that with increasing bubble size the fluctuation range increases and higher shear stress values are more likely to occur. Nevertheless it is clear that due to the 2 s time interval that is taken into account here, the general occurring shear stress is dominated by the single phase flow which is emphasized by the fact that the median shear stress is constant for one channel depth independently of the bubble size.

Fig.5b has clear and evident tendencies. Looking at the probability range '1%-10%' the effect mentioned above is obvious again. For all cases this range is very small in comparison to the other ranges, and looking at one channel depth and different bubble size the shear stress range that is related to this probability range is constant. This is due to the steep slope in the CDF at the shear stress value generated by the single phase flow (as can be found in Fig.2c). Looking at a constant bubble size, an increase of the channel depth leads to a decrease of the shear stress fluctuation range. This is due to the lower grade of confinement. This was the effect that also leads to an increase of the shear stress range in the probability range '10%-90%' i.e. the slopes get less steep. Especially for the cases with a bubble size smaller than the channel depth, the more emphasized three-dimensional oscillation mentioned above is responsible for this effect. Looking at one channel depth and an increasing bubble size, an increase of the shear stress fluctuation ranges is evident. The larger the bubble, the stronger is its influence on the flow and the more wide the bubble induced shear stresses will be spread.

In Fig.5a the conditions are more complicated partly due to the problems with the calibration mentioned above and also since there is no superimposed liquid flow influencing the data. Regarding the overall range of shear stresses, for a 3 mm bubble the tendencies are according to the tendencies with liquid velocity. With increasing channel depth the total fluctuation range decreases due to the lower grade of confinement. For a channel depth of 3 mm and varying bubble size and a channel depth of 5mm and the bubble sizes 3-5 mm the tendencies are also comparable to the ones mentioned above. With increasing bubble size the shear stress ranges that are related to the probability ranges increase. From the point at which the bubble size is equal or larger than the channel depth the slope of the CDF curves increases. All other tendencies mentioned above for Fig.5b are not as clear in Fig.5a. Several reasons can be addressed here to explain this behavior. The major reason is the fact that no liquid flow is obliterating the influence of the bubble. As known from Prieske et al. [1] without liquid flow several eddies are apparent in the Kármán-vortex-street-like wake of the bubble. Unpublished results generated with particle image velocimetry showed that each eddy grows with time at a stable location. For superimposed liquid flows, depending on the liquid velocity, these eddies either do not appear at all as there is no oscillating movement or they are dampened. This leads to a much slower stabilization of the flow in comparison to parameter combinations with superimposed liquid velocity. The author's experience is that with superimposed liquid velocity a stabilization of the flow is apparent approximately 2 seconds after the bubble passed by. Without superimposed liquid velocity, the influence of the bubble on the flow can be observed for more than 15 seconds.

Figure 6a (without superimposed liquid velocity) and 6b (with superimposed liquid velocity) show the median values of the generally occurring shear stress and their occurrence in the CDF as described in Fig.2c for every parameter combination that was tested with the data being processed using equation (2). For most of the parameter combinations the tendencies stay the same as in Fig.5a and 5b but as seen before, the correction leads to an increase of the shear stress ranges in general and by that it leads to an increase of the different probability ranges but the medians are almost not affected by the transient correction.

Generally, the values are in the same range the average values found by Bérubé's group, with values from 0.07 Pa to 1.24 Pa [3] and 0.3 Pa to 0.7 Pa [4], respectively.

4. Conclusions

A statistical analysis of the shear stress generated by single bubbles was shown for 21 different parameter combinations and 40000 single bubble rises. This large amount of data was used as a data base for different types of analysis. The maximum shear stresses and the global shear stress levels where the latter represent the global shear stress fluctuations were determined. To the authors' knowledge, for the first time in membrane research a transient correction of the EDM data was performed which is necessary in cases of highly transient processes. The transient corrected values shown here are mostly closer to the CFD values in earlier publications and therefore their higher quality can be considered.

By showing different probability ranges gained from cumulative distribution functions in a bar plot, a way of presenting the data was introduced that simplifies the comparison between the different parameter combinations. Additionally, this type of diagram offers a very comprehensive overview of the measured data.

The determination of the maximum shear stress values and their according probability ranges showed that without superimposed liquid velocity, the highest median value was obtained for a channel depth of 7 mm and a bubble size of 9 mm with appr. 1.5 Pa (steady analysis) or 3 Pa (transient corrected analysis) respectively. With superimposed liquid velocity, the highest value was obtained for a channel depth of 5mm and a bubble size of 9 mm with appr. 1.3 Pa (steady analysis) or 4.7 Pa (transient corrected analysis) respectively.

The determination of the global shear stress level representing the fluctuations induced by the bubble showed that without superimposed liquid velocity, the largest probability range (1% to 99%) was obtained for a channel depth of 7 mm and a bubble size of 9 mm with values from appr. 0-1.3 Pa (steady analysis) or 0-2 Pa (transient corrected analysis) respectively. With superimposed liquid velocity, the largest probability range (1% to 99%) was obtained for a channel depth of 5 mm and a bubble size of 9 mm with values from appr. 0.2-1.1 Pa (steady analysis) or 0-2.6 Pa (transient corrected analysis) respectively.

As an additional liquid flow is preferable for the operation of MBRs anyway, regarding the results shown here a channel depth of 5 mm and a bubble size larger than the channel depth shows the most promising results.

Acknowledgements

Financial support by DAAD D/10/46059, DFG KR 1639/18-1 and DFG SFB/TR63 InPROMPT is gratefully acknowledged. Special thanks for the support during this work go to Andrea Hasselmann, Alexander Fleck, Tim Karsten, Nikolay Kolev and Jan-Paul Ruiken.

References

[1] H. Prieske, L. Böhm, A. Drews, M. Kraume, Optimised hydrodynamics for membrane bioreactors with immersed flat sheet membrane modules, Desalin. Water Treat. 8, 1-3 (2010) 270 – 276.

[2] L. Böhm, A. Drews, H. Prieske, P. Bérubé, M. Kraume, The importance of fluid dynamics for MBR fouling mitigation, Bioresour. Technol. 122 (2012) 50 – 61.

[3] P.R. Bérubé, G. Afonso, F. Taghipour, C.C.V. Chan, Quantifying the shear at the surface of submerged hollow fiber membranes, J. Membr. Sci. 279, 1-2 (2006) 495 – 505.

[4] C.C.V. Chan, P.R. Bérubé, E.R. Hall, Shear profiles inside gas sparged submerged hollow fiber membrane modules, J. Membr. Sci. 297, 1-2 (2007) 104 – 120.

[5] B.G. Fulton, J. Redwood, M. Tourais, P.R. Bérubé, Distribution of surface shear forces and bubble characteristics in full-scale gas sparged submerged hollow fiber membrane modules, Desalination 281 (2011) 128 – 141.

[6] B.G. Fulton, P.R. Bérubé, Optimizing the sparging condition and membrane module spacing for a ZW500 submerged hollow fiber membrane system, Desalin. Water Treat., 42, 1-3 (2012) 8–16.

[7] N. Ratkovich, C.C.V. Chan, P.R. Bérubé, I. Nopens, Experimental study and cfd modelling of a two-phase slug flow for an airlift tubular membrane, Chem. Eng. Sci. 64, 16 (2009) 3576 – 3584.

[8] N. Ratkovich, C. C. V. Chan, P. R. Bérubé, I. Nopens, Investigation of the effect of viscosity on slug flow in airlift tubular membranes in search of a sludge surrogate, Water Sci. Technol. 61, 7 (2010) 1801–1809.

[9] N. Ratkovich, C. C. V. Chan, P. R. Bérubé, I. Nopens, Analysis of shear stress and energy consumption in a tubular airlift membrane system, Water Sci. Technol. 64, 1 (2011) 189–198.

[10] N. Ratkovich, P.R. Bérubé, I. Nopens, Assessment of mass transfer coefficients in coalescing slug flow in vertical pipes and applications to tubular airlift membrane bioreactors, Chem. Eng. Sci. 66, 6 (2011) 1254–1268.

[11] G. Ducom, F.-P. Puech, C. Cabassud, Air sparging with flat sheet nanofiltration: a link between wall shear stresses and flux enhancement, Desalination 145, 1-3 (2002) 97 – 102.

[12] G. Ducom, F.-P. Puech, C. Cabassud, Gas/liquid two-phase flow in a flat sheet filtration module: Measurement of local wall shear stresses, Can. J. Chem. Eng. 81, 3-4 (2003) 771–775.

[13] K. Zhang, Z. Cui, R.W. Field, Effect of bubble size and frequency on mass transfer in flat sheet MBR, J. Membr. Sci. 332, 1-2 (2009) 30–37.

[14] C. Gaucher, P. Jaouen, J. Comiti, P. Legentilhomme, Determination of cake thickness and porosity during cross-flow ultrafiltration on a plane ceramic membrane surface using an electrochemical method, J. Membr. Sci. 210, 2 (2002) 245 – 258.

[15] C. Gaucher, P. Legentilhomme, P. Jaouen, J. Comiti, J. Pruvost, Hydrodynamics study in a plane ultrafiltration module using an electrochemical method and particle image velocimetry visualization, Exp. Fluids 32 (2002) 283–293.

[16] C. Gaucher, P. Legentilhomme, P. Jaouen, J. Comiti, Influence of fluid distribution on the wall shear stress in a plane ultrafiltration module using an electrochemical method, Chem. Eng. Res. Des. 80, 1 (2002) 111 – 120.

[17] C. Gaucher, P. Jaouen, P. Legentilhomme, J. Comiti, Suction effect on the shear stress at a plane ultrafiltration ceramic membrane surface, Sep. Sci. Technol. 37, 10 (2002) 2251–2270.

[18] C. Gaucher, P. Jaouen, P. Legentilhomme, J. Comiti, Influence of fluid distribution on the ultrafiltration performance of a ceramic flat sheet membrane, Sep. Sci. Technol. 38, 9 (2003) 1949–1962.

[19] V. Sobolik, J. Tihon, O. Wein, K. Wichterle, Calibration of electrodiffusion friction probes using a voltage-step transient, J. Appl. Electrochem. 28 (1998) 329–335.

[20] V. Sobolik, O. Wein, J. Cermak, Simultaneous measurement of film thickness and wall shear-stress in wavy flow of non-newtonian liquids, Collect. Czech. Chem. Commun. 52, 4 (1987) 913–928.

[21] O. Wein, V.V. Tovcigrecko, V. Sobolik, Transient convective diffusion to a circular sink at finite peclet number, Int. J. Heat Mass Transfer 49, 23-24 (2006) 4596 – 4607.

[22] J. Tihon, V. Tovchigrechko, V. Sobolik, O. Wein, Electrodiffusion detection of the near-wall flow reversal in liquid films at the regime of solitary waves, J. Appl. Electrochem. 33 (2003) 577–587.

[23] L. Philip Reiss, Thomas J. Hanratty, Measurement of instantaneous rates of mass transfer to a small sink on a wall, AIChE J. 8, 2 (1962) 245–247.

[24] N.V. Ndinisa, A.G. Fane, D.E. Wiley, D.F. Fletcher, Fouling control in a submerged flat sheet membrane system: Part II - two phase flow characterization and CFD simulations, Sep. Sci. Technol. 41, 7 (2006) 1411–1445.

Tab.1. Investigated parameter combinations where '--' indicates parameter combinations that were not investigated either due to the fact that no flow occurs or the bubble was not stable and broke up

Fig. 1. Schematic of the rectangular channel (a) and flow sheet of the experimental system (b)

Fig. 2. Shear stress data over time of three sensors for one bubble (7mm channel depth, 5mm bubble, 0.2m/s superimposed liquid velocity) with the maximum shear stress marked with a black **o** (a) the CDF plots based on 1500 bubble rises of the maximum shear stress (b) and of the global shear stress level (c) (median marked with a white **x**)

Fig. 3. Comparison of the probability ranges of the occurring maximum shear stresses for the parameter combinations without (a) and with superimposed liquid velocity (b) (steady analysis)

Fig. 4. Comparison of the probability ranges of the occurring maximum shear stresses for the parameter combinations without (a) and with superimposed liquid velocity (b) (transient corrected analysis)

Fig. 5. Comparison of the probability ranges of the global shear stress level for the parameter combinations without (a) and with superimposed liquid velocity (b) (steady analysis)

Fig. 6. Comparison of the probability ranges of the global shear stress level for the parameter combinations without (a) and with superimposed liquid velocity (b) (transient corrected analysis)

Tab.1. Investigated parameter combinations where '--' indicates parameter combinations that were not investigated either due to the fact that no flow occurs or the bubble was not stable and broke up

channel depth [mm]		3		5		7	
liquid velocity [cm/s]		0	20	0	20	0	20
bubble size [mm]	0	--	+	--	+	--	+
	3	+	+	+	+	+	+
	5	+	+	+	+	+	+
	7	+	--	+	+	+	+
	9	--	--	+	+	+	+

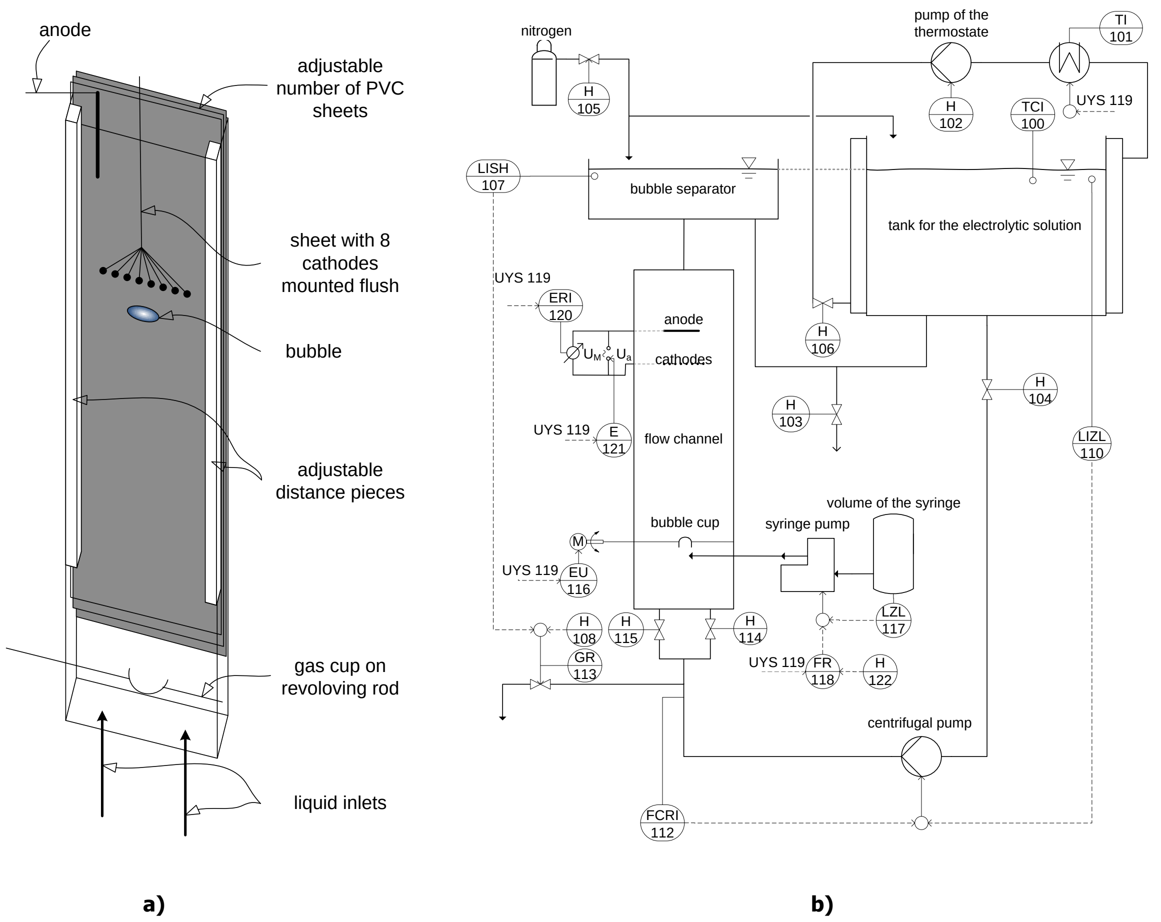

Fig. 1. Schematic of the rectangular channel (a) and flow sheet of the experimental system (b)

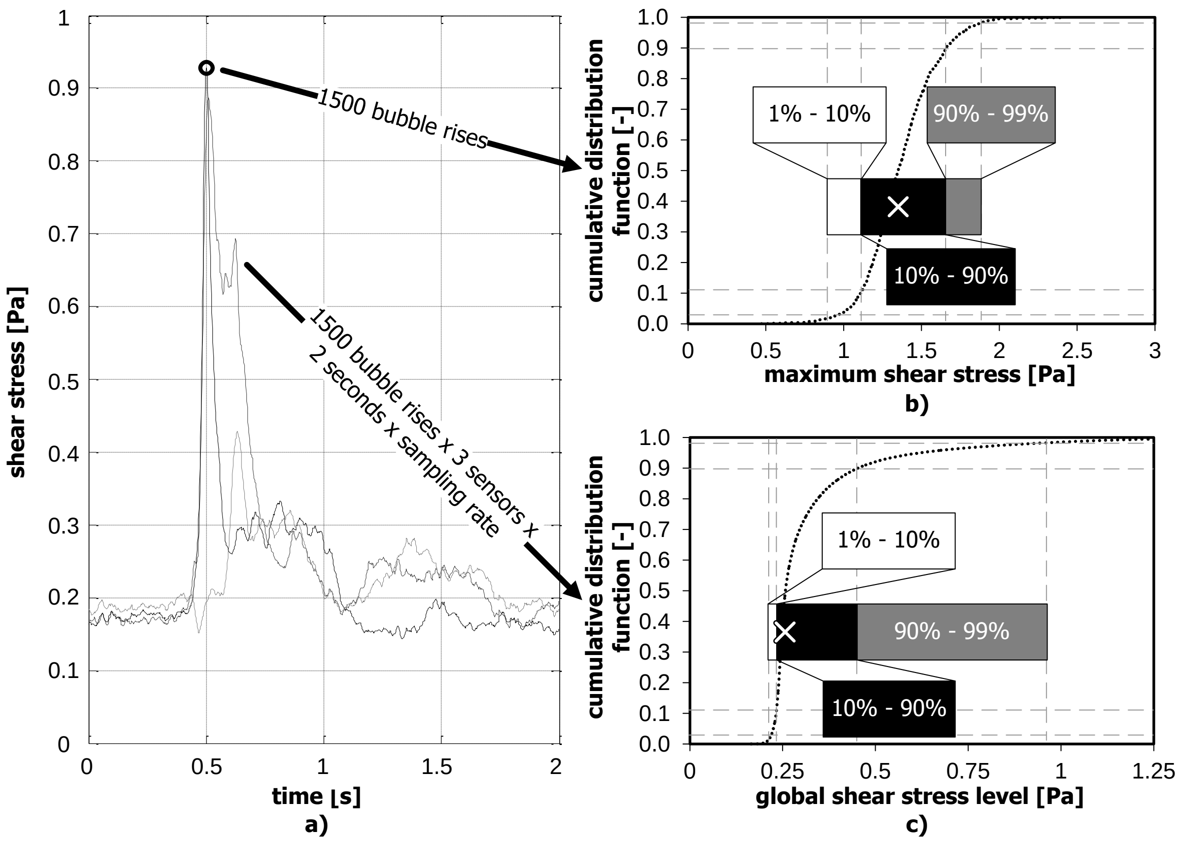

Fig. 2. Shear stress data over time of three sensors for one bubble (7mm channel depth, 5mm bubble, 0.2m/s superimposed liquid velocity) with the maximum shear stress marked with a black **o** (a) the CDF plots based on 1500 bubble rises of the maximum shear stress (b) and of the global shear stress level (c) (median marked with a white **x**)

1

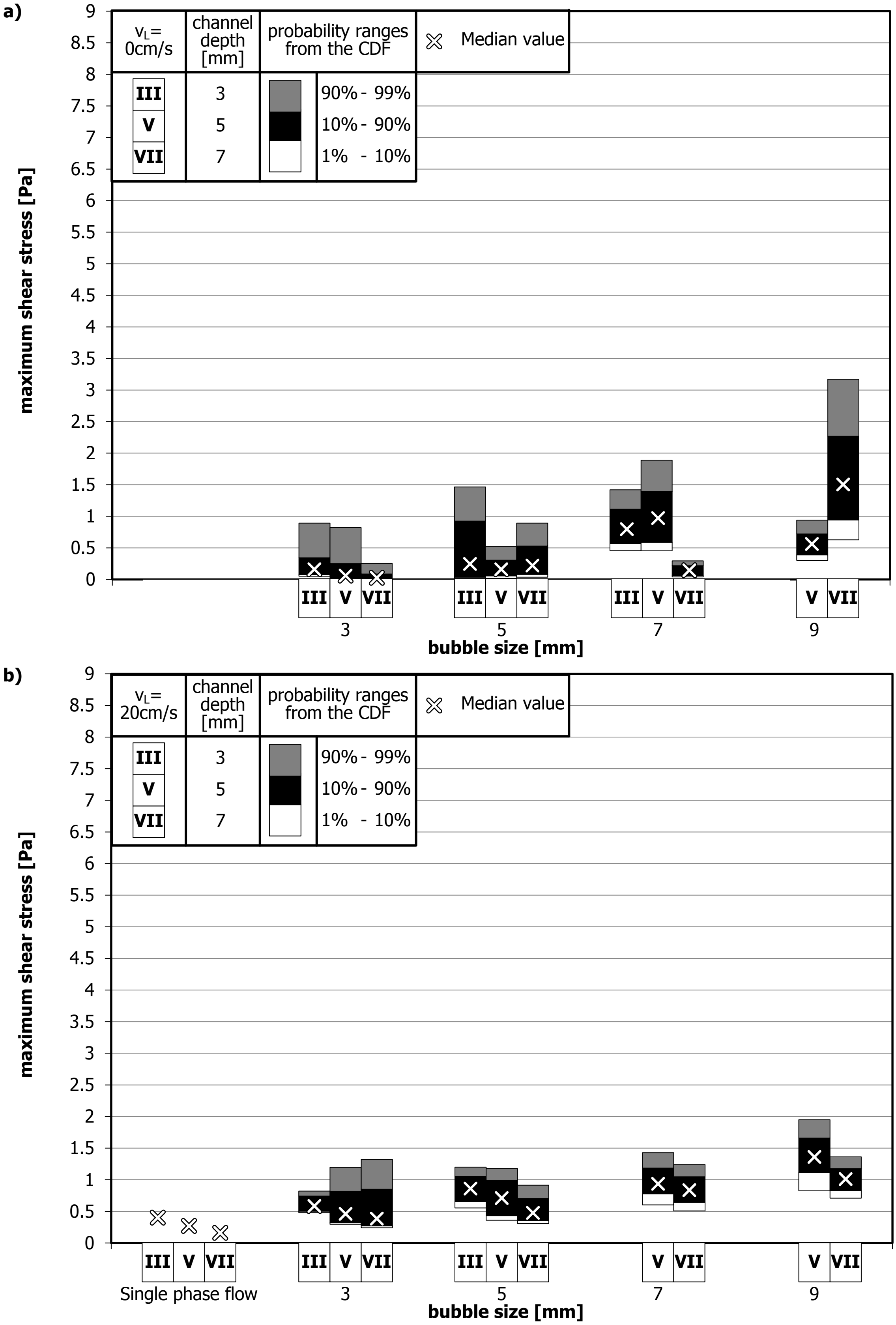

Fig. 3. Comparison of the probability ranges of the occurring maximum shear stresses for the parameter combinations without (a) and with superimposed liquid velocity (b) (steady analysis)

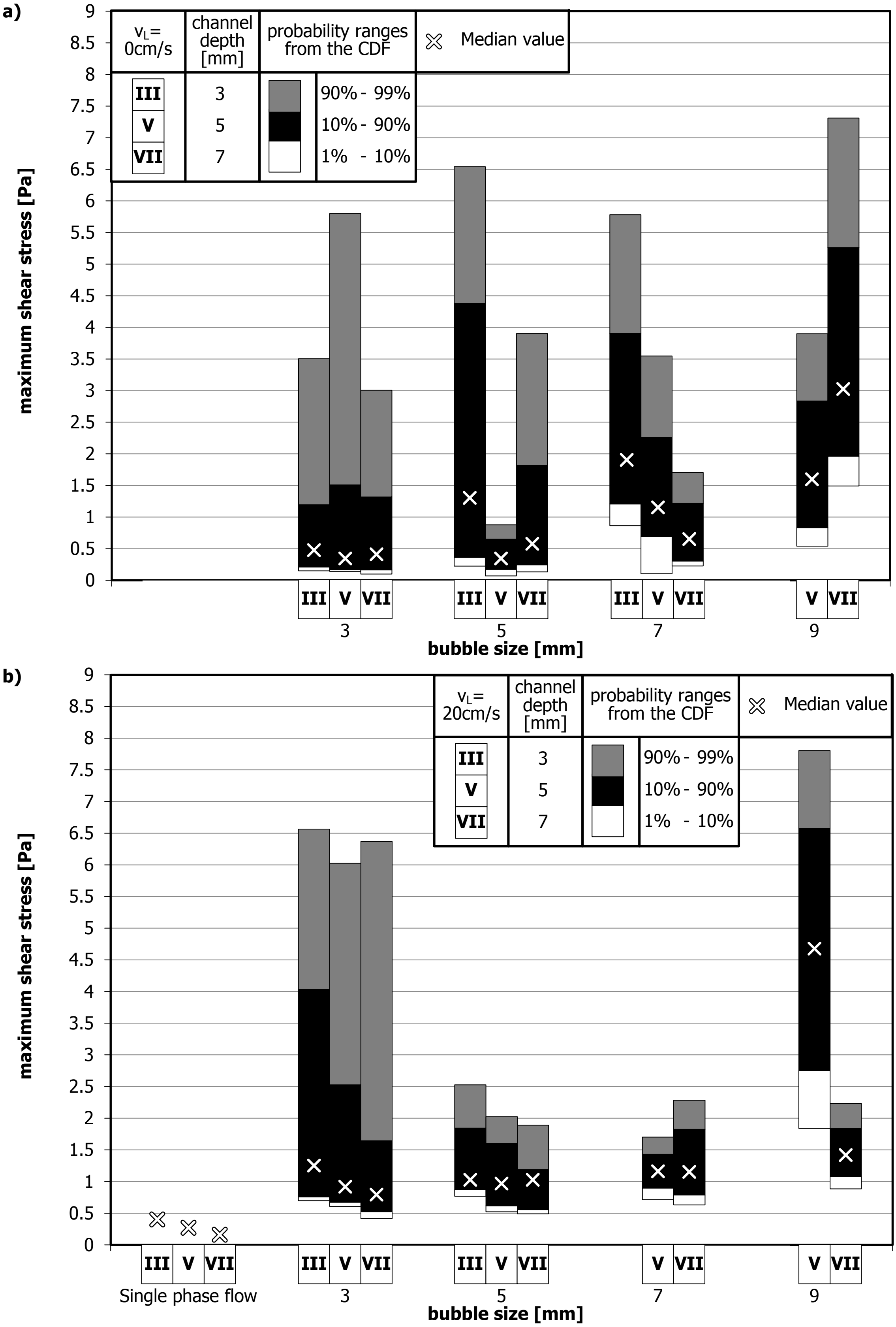

Fig. 4. Comparison of the probability ranges of the occurring maximum shear stresses for the parameter combinations without (a) and with superimposed liquid velocity (b) (transient corrected analysis)

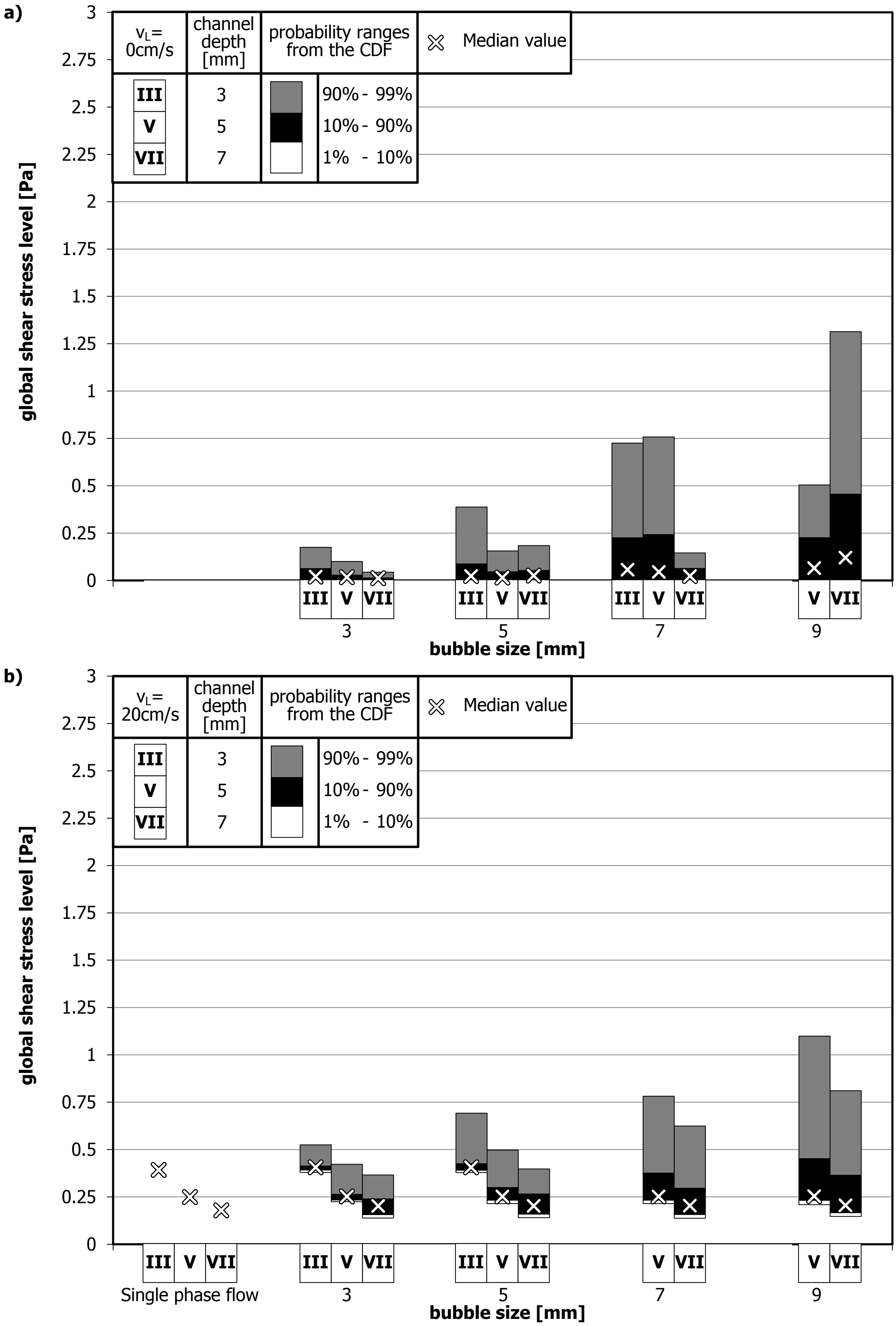

Fig. 5. Comparison of the probability ranges of the global shear stress level for the parameter combinations without (a) and with superimposed liquid velocity (b) (steady analysis)

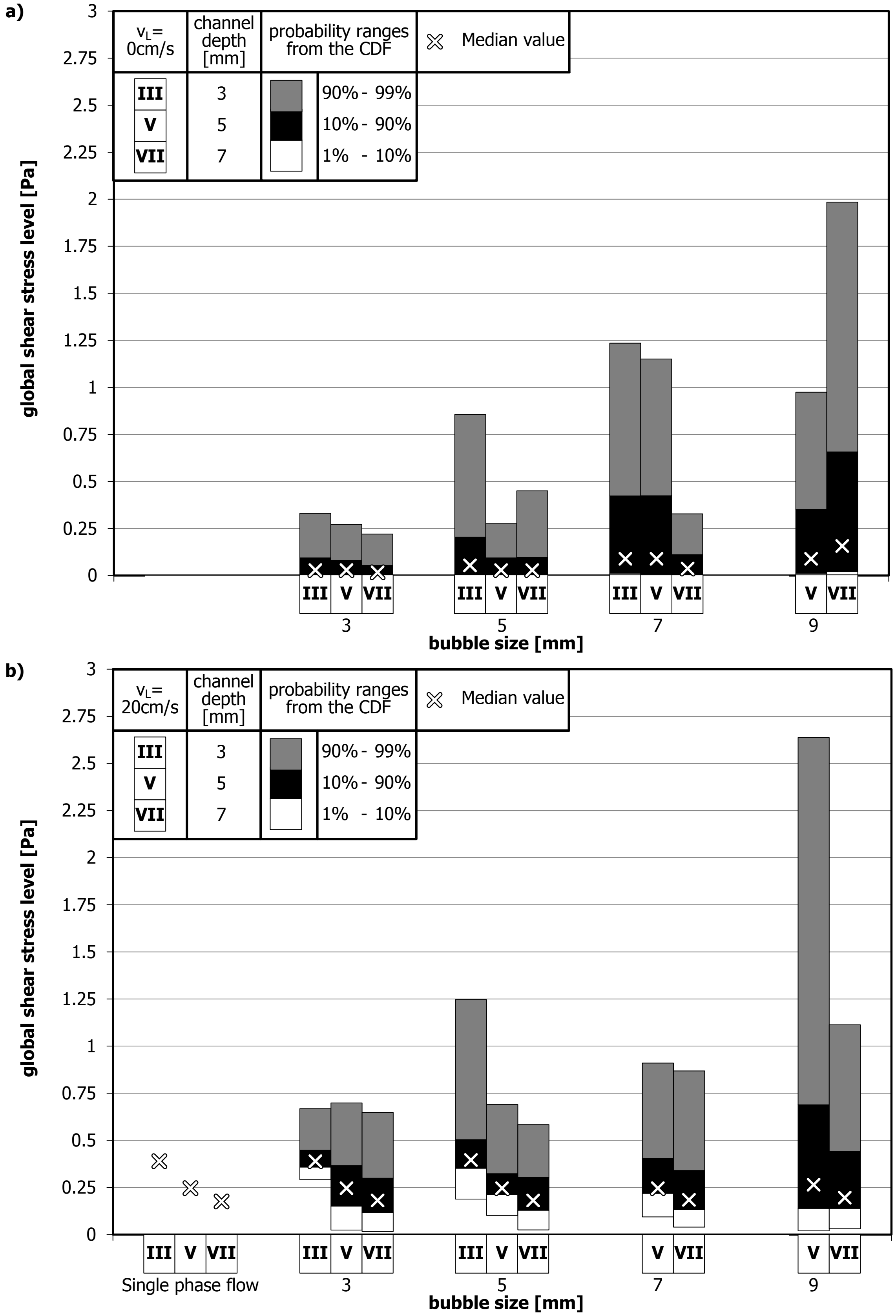

Fig. 6. Comparison of the probability ranges of the global shear stress level for the parameter combinations without (a) and with superimposed liquid velocity (b) (transient corrected analysis)